Kinetics and Mechanisms of Hydrogen Peroxide Disproportionation Catalyzed by Mononuclear Schiff Base Manganese(III) Complexes: Effects of Chelate and Hydroxide Ion on Hydrogen Peroxide Disproportionation in *N,N*-Dimethylformamide

Minori Uehara, Mika Urade, and Yuriko Abe*

Department of Chemistry, Faculty of Science, Nara Women's University, Nara 630

(Received August 25, 1997)

The preparation of [Mn(saltnOCOPh)Cl]·DMF (H_2saltnOCOPh: *N,N'*-(2-benzoyloxypropane-1,3-diyl)bis(salicylideneamine)) and kinetics and mechanisms of H_2O_2 disproportionation catalyzed by mononuclear Schiff base manganese(III) complexes, such as [Mn(salen)Cl] (H_2salen: *N,N'*-ethylenebis(salicylideneamine)), [Mn(saltn)Cl] (H_2saltn: *N,N'*-propane-1,3-diylbis(salicylideneamine)), [Mn(saltnOH)Cl] (H_2saltnOH: *N,N'*-(2-hydroxypropane-1,3-diyl)bis(salicylideneamine)), and [Mn(saltnOCOPh)Cl] in *N,N*-dimethylformamide (DMF), have been investigated. The disproportionation of H_2O_2 to O_2 and H_2O proceeds coupled with the redox cycle between the Mn(III) complex and the Mn(IV) intermediate: the first step is the fast equilibrium (K_m) of the Mn(III) complex and the Mn(IV) intermediate formed by the reaction of the Mn(III) complex with H_2O_2, followed by a slow reaction (k_1) of the Mn(IV) intermediate with H_2O_2 to produce O_2 and H_2O recovering the original Mn(III) complex. The K_m values decrease in the following order: [Mn(salen)-Cl] (728 $mol^{-1}\,dm^3$)$\gg$[Mn(saltnOH)Cl] (28.0 $mol^{-1}\,dm^3$) > [Mn(saltn)Cl] (6.28 $mol^{-1}\,dm^3$) > [Mn(saltnOCOPh)Cl] (1.83 $mol^{-1}\,dm^3$), reflecting an increased distortion along the axis containing the coordination of H_2O_2 to the Mn(III) complex. On the other hand, the rate constants (k_1) fall into the following sequences: [Mn(saltnOH)Cl] (4.29×10^5 $mol^{-2}\,dm^6\,s^{-1}$) > [Mn(salen)Cl] (1.67×10^5 $mol^{-2}\,dm^6\,s^{-1}$) > [Mn(saltnOCOPh)Cl] (3.34×10^4 $mol^{-2}\,dm^6\,s^{-1}$) > [Mn-(salen)Cl] (6.15×10^3 $mol^{-2}\,dm^6\,s^{-1}$). In spite of the small K_m values for saltnOH, saltnOCOPh, and saltn complexes with the 1,3-diamine ligand, compared to that for the salen complex, the large k_1 value for the saltnOH complex strongly suggests stabilization of the transition state for the formation of hydrogen-bondings among the Mn(IV) intermediates and H_2O_2. Futhermore, the effect of the OH^- ion on the H_2O_2 disproportionation catalyzed by [Mn(salen)Cl] has been reported. On account of the formation of [Mn(salen)OH] coordinated by the OH^- ion, the appearance of the reaction path involving not only the Mn(III)–Mn(IV) cycle, but also the Mn(II)–Mn(III) cycle, is shown based on the ESR and visible spectral studies. The activity for the Mn(II)–Mn(III) cycle is 20 times larger than that for the Mn(III)–Mn(IV) cycle.

Manganese is an essential element in many biological processes, where manganese-containing enzymes exhibit two distinguished functions: a Lewis acid and a redox catalyst.[1] On account of the strong affinity of manganese ion to oxygen atom coupled with its redox process, manganese-containing enzymes catalyze the oxidation of water in photosystem II[2] and disproportionation of the superoxide ion[3] and hydrogen peroxide.[4] Among them, manganese catalase (Mn-CAT) mediates the disproportionation of hydrogen peroxide to dioxygen and water in biological systems.[4] Mn-CAT's are also of interest in concerning their functional resemblance to oxygen evolving complex in the photosynthetic reaction center of green plants. Mn-CAT's have been found in three different origins: *Lactobacillus plantarum*,[4a,4b] *Thermus thermophilus*,[4c] and *Thermoleophilum album*.[4d] For the first two Mn-CAT's, the presence of the dinuclear manganese core structure has been shown based on X-ray structure analysis,[5] electron paramagnetic resonance,[6] and extended X-ray absorption fine studies;[7] however, the detailed structure of the active site and reaction mechanism are still unknown. In parallel with these studies, syntheses and the catalase-like activities of dinuclear manganese complexes as functional models of these active sites have been reported, allowing a comparison to the characterized systems.[8—18]

In this paper we report on the preparation and characterization of [Mn(saltnOCOPh)Cl]·DMF (H_2saltnOCOPh: *N,N'*-(2-benzoyloxypropane-1,3-diyl)bis(salicylideneamine)) and kinetics and mechanisms of hydrogen peroxide disproportionation catalyzed by mononuclear Schiff base manganese-(III) complexes, such as [Mn(salen)Cl] (H_2salen: *N,N'*-ethylenebis(salicylideneamine)), [Mn(saltn)Cl] (H_2saltn: *N,N'*-propane-1,3-diylbis(salicylideneamine)), [Mn(saltnOH)Cl] (H_2saltnOH: *N,N'*-(2-hydroxypropane-1,3-diyl)bis(salicylideneamine)), and [Mn(saltnOCOPh)Cl] in *N,N*-dimethylformamide (DMF), as shown in Fig. 1. When mononuclear Schiff base manganese complexes are employed in hydrogen peroxide disproportionation, it is expected that dinuclear manganese complexes bridged by hydrogen peroxide will be formed in the intermediate and/or transition state, owing to the strong affinity of oxygen atom to manganese complexes and the moderate redox potentials of manganese complexes. Thus, although the Mn–Mn distance is fixed in the interme-

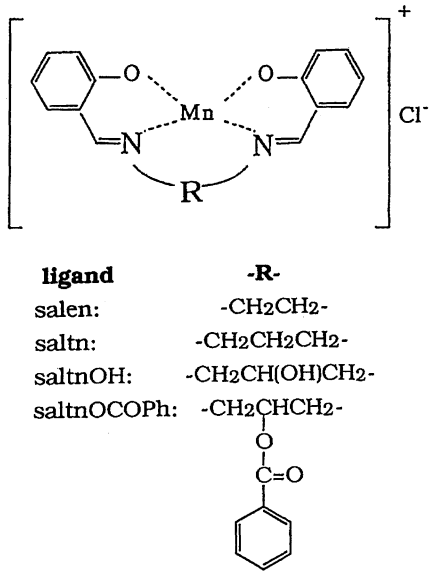

Fig. 1. Structures of [Mn(salen)Cl], [Mn(saltn)Cl], [Mn(saltnOH)Cl], and [Mn(saltnOCOPh)Cl] in DMF.

diate and/or the transition state, the structures of the H_2O_2 adduct in the intermediate and/or the transition state may be similar to those of dinuclear manganese complexes utilized as the catalyst. The use of mononuclear manganese complexes also provides basic information with which to develop synthetic model manganese compounds that mimic the properties of living systems. In the present work, mononuclear Mn(III) complexes, such as [Mn(salen)Cl], [Mn(saltn)Cl], [Mn(saltnOH)Cl], and [Mn(saltnOCOPh)Cl], as catalysts were used to clarify the chelate effect on H_2O_2 disproportionation. Although the salen donor atoms and salen framework of the [Mn(salen)Cl] complex are coplanar to each other,[19] the other complexes with 1,3-diamine ligands may have a distortion based on the six-membered ring on the 1,3-diamine moiety.[8,20] It has been pointed out that the small activities for synthetic manganese complexes as functional modes, compared to the large activities for Mn-CAT's, are due to the lack of proton donor and acceptor groups near to the catalytic site.[13] Thus, [Mn(saltnOCOPh)Cl] complex with a proton acceptor group was newly prepared. Hydrogen-bonding formation between saltnOH and saltnOCOPh complexes and H_2O_2 would be expected. Furthermore, the effect of the hydroxide ion on H_2O_2 disproportionation by [Mn(salen)Cl] was investigated in DMF.

Experimental

Preparation of [Mn(saltnOCOPh)Cl]·DMF. Schiff base complex, [Mn(salen)Cl] was prepared as described.[21] [Mn(saltn)Cl] and [Mn(saltnOH)Cl] complexes were prepared by modifying the method of Bonadies et al.[20] The preparation of [Mn(saltnOCOPh)Cl]·DMF was carried out as follows: [Mn(saltnOH)Cl] (0.77 g, 0.002 mol) was dissolved in a CH_3CN–DMF (2 : 1 v/v) mixture (20 cm^3) in the presence of benzoic anhydride (0.9 g, 0.004 mol) and 4-*N*,*N*-dimethylaminopyridine (0.24 g, 0.002 mol). After stirring at room temperature for 2 d, the solution was evaporated, and a dark green powder was obtained by adding diethyl ether. An analytical pure sample obtained by passing on Sephadex LH-20 (eluent: CH_3OH) was used for characterization by elemental analysis, absorption spectra, infrared spectra, cyclic voltammometry, and conductivity measurements. Calcd for [Mn $C_{24}H_{20}N_2O_4Cl$]·DMF: C, 57.50; H, 4.79; N, 7.45%. Found: C, 57.28; H, 4.81, N, 7.52%.

Materials for Kinetic Studies. Hydrogen peroxide and potassium permanganate were used without further purification. Tetra-*n*-butylammonium hydroxide DMF solution was prepared by dissolving tetra-*n*-butylammonium hydroxide in a DMF solvent after the CH_3OH in tetra-*n*-butylammonium hydroxide CH_3OH solution was removed by evaporation. Tetra-*n*-butylammonium perchlorate was recrystallized from ethanol. DMF was purified as described.[22]

Physical Measurements. Infrared and UV spectra were recorded on a JASCO FT/IR-8900μ spectrophotometer using KBr disks and a Shimadzu UV-3100 spectrophotometer, respectively. Molar conductances were measured with a Yanagimoto MY-8 conductivity meter at room temperature. Cyclic voltammograms were recorded by using a Hokuto Denko HZ-1A apparatus. Measurements were carried out in a DMF solution (1×10^{-3} mol dm^{-3}) containing tetra-*n*-butylammonium perchlorate (0.1 mol dm^{-3}) as the supporting electrolyte. A three-electrode cell was used which was equipped with a glassy carbon working cell, a platinum as the counter electrode, and a Ag/$AgPF_6$ electrode as the reference. ESR spectra were recorded on a JEOL RE-3X ESR spectrometer on frozen DMF solution at liquid nitrogen temperature. The evolution of dioxygen in DMF was detected by using a DKK HDO-110 oxygen meter.

Kinetic Studies on H_2O_2 Disproportionation. The H_2O_2 disproportionation catalyzed by the Mn(III) complex at 25 °C was followed by a decrease in the H_2O_2 concentration by titration with a $KMnO_4$ solution after passing aliquots of the reaction solution through a cation ion-exchange resin (Dowex 50×8, 50—100 mesh) at regular time intervals. The evolved dioxygen was measured with a percentage saturation of oxygen: The oxygen concentrations of the DMF solution saturated with air and the air-free DMF solution was taken to be 100 and 0 percentage, respectively. The ionic strength was adjusted to 0.01 mol dm^{-3} with tetra-*n*-butylammonium perchlorate.

Results and Discussion

Characterization of [Mn(saltnOCOPh)Cl]·DMF. The infrared spectrum of [Mn(saltnOCOPh)Cl]·DMF on KBr disks exhibited a new intense band at 1717 cm^{-1} due to the replacement of a hydroxy group by a benzoyloxy group on the 1,3-diamine ring. The corresponding band for [Cu(saltnOCOPh)], as proved by X-ray crystallography, is shown at 1722 cm^{-1}.[23] Conductivity studies have revealed that [Mn(saltnOCOPh)Cl] as well as [Mn(salen)Cl], [Mn(saltn)Cl], and [Mn(saltnOH)Cl] behaves as a 1 : 1 electrolyte in DMF, indicating no coordination of Cl^- to the Mn(III) ion. [Mn(saltnOCOPh)Cl] in DMF shows an intense absorption band at 378 nm ($\log\varepsilon$ (mol^{-1} dm^3 cm^{-1}) = 3.70) similar to [Mn(saltn)Cl] at 377 nm ($\log\varepsilon$ = 3.83) and [Mn(saltnOH)Cl] at 378 nm ($\log\varepsilon$ = 3.81), which is assigned to the π–π^* transition associated with an azomethine linkage,[24,25] whereas [Mn(salen)Cl] in DMF shows the corresponding band at 400 nm ($\log\varepsilon$ = 3.67). Each complex exhibits a visible band with a moderate intensity near to 570 nm in DMF assigned to a d–d band of the Mn(III) ion. The cyclic voltammogram of [Mn(saltnOCOPh)Cl] revealed one reversible redox wave at $E_{1/2}$ = −0.53 V vs. Ag/$AgPF_6$ and one quasireversible redox

wave near to +0.5 V vs. Ag/$AgPF_6$ in DMF, corresponding to the Mn(III)/Mn(II) and Mn(IV)/Mn(III) redox processes, respectively, which are similar to those of [Mn(salen)Cl], [Mn(saltn)Cl], and [Mn(saltnOH)Cl], as shown in Table 1.

Chelate Effect on H_2O_2 Disproportionation. The time courses of the H_2O_2 concentration and the O_2 evolution in the presence of [Mn(salen)Cl] are shown in Figs. 2 and 3 as an example, with essentially similar data obtained for the other complexes. These results indicate that mononuclear Schiff base manganese complexes catalytically mediate the disproportionation of H_2O_2 to O_2 and H_2O in DMF. The addition of acrylonitrile as a radical scavenger to the system, which proceeds by the radical reaction, significantly affects the reaction.[26] In the present investigation, the reactions were little affected by acrylonitrile. Thus, H_2O_2 disproportionation catalyzed by the Mn(III) complex does not include the formation of radical species. The initial rates (v_0) are proportional to the second order in the Mn(III) concentration, as shown in Fig. 4. Figure 5 shows the spectral changes in H_2O_2 disproportionation by [Mn(salen)Cl] in DMF. In the early stage of the reaction until 10 min, fast increases in the absorbance with an intense intensity in the 500—600 nm range are seen in H_2O_2 disproportionation. In the visible region, no prominent absorption is seen for Mn(II) complexes with a high-spin d^5 electron configuration. Thus, the increased absorbances may be based on a ligand-to-metal charge transfer (LMCT) in the Mn(IV) intermediate, which is attributed

Table 1. The Equilibrium Constants (K_m), Rate Constants (k_1), and Redox Potentials ($E_{1/2}$ for Mn(III)–Mn(II)) for [Mn(salen)Cl], [Mn(saltnOH)Cl], [Mn(saltnOCOPh)-Cl], and [Mn(saltn)Cl][a]

Ligand	K_m	k_1	$E_{1/2}$
	$mol^{-1}dm^3$	$10^5\ mol^{-2}\ dm^6 s^{-1}$	V vs. Ag-$AgPF_6$
salen	728±50	1.67±0.10	−0.56
saltnOH	28.0±2.2	4.29±0.60	−0.54
saltnOCOPh	1.83±0.10	0.334±0.010	−0.53
saltn	6.28±0.41	0.0615±0.0063	−0.55

a) The uncertainty is the standard deviation.

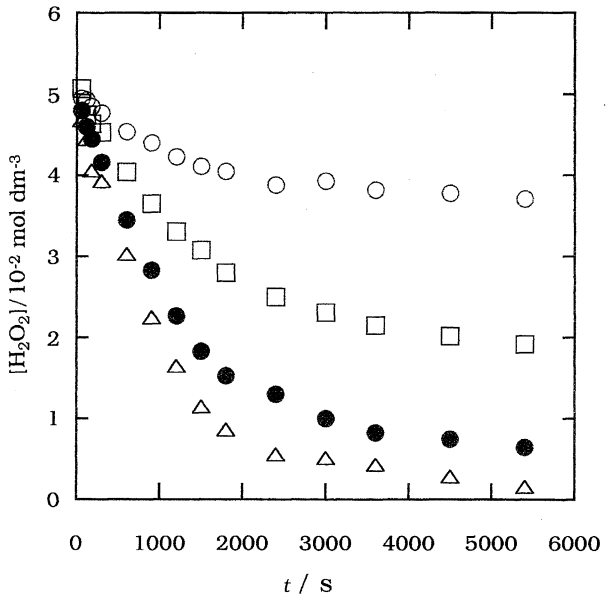

Fig. 2. Time courses of the H_2O_2 disproportionation catalyzed by [Mn(salen)Cl] in DMF at 25 °C. $[H_2O_2]_0 = 5.00\times10^{-2}$ mol dm^{-3}, $[[Mn(salen)Cl]]_0/10^{-4}$ mol dm^{-3}: (○); 0.25, (□); 0.50, (●); 0.75, (△); 1.00.

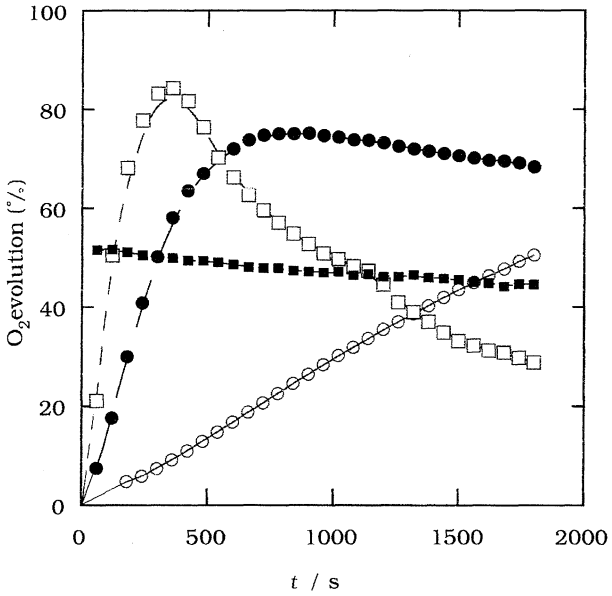

Fig. 3. Time courses of O_2 evolution in the H_2O_2 disproportionation catalyzed by [Mn(salen)Cl] in the absence and presence of the OH^- ion in DMF at 25 °C. $[H_2O_2]_0 = 5.00\times10^{-3}$ mol dm^{-3}, $[[Mn(salen)Cl]]_0 = 2.00\times10^{-4}$ mol dm^{-3}, $[OH^-]_0/10^{-4}$ mol dm^{-3}: (○); 0, (●); 0.60, (□); 1.20, (■); 4.90.

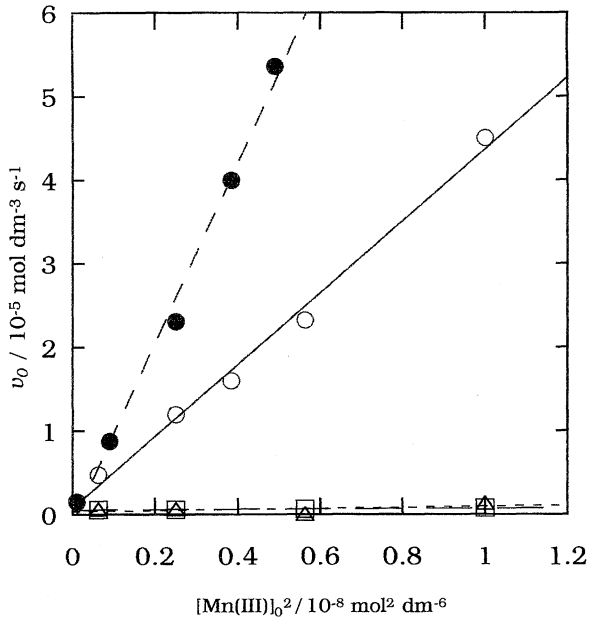

Fig. 4. The plots of v_0 vs. $[Mn(III)]_0^2$. $[H_2O_2]_0 = 5.00\times10^{-2}$ mol dm^{-3}, (○) : [Mn(salen)Cl]; (△) : [Mn-(saltn)Cl]; (●) : [Mn(saltnOH)Cl]; (□) : [Mn(saltnOCOPh) Cl].

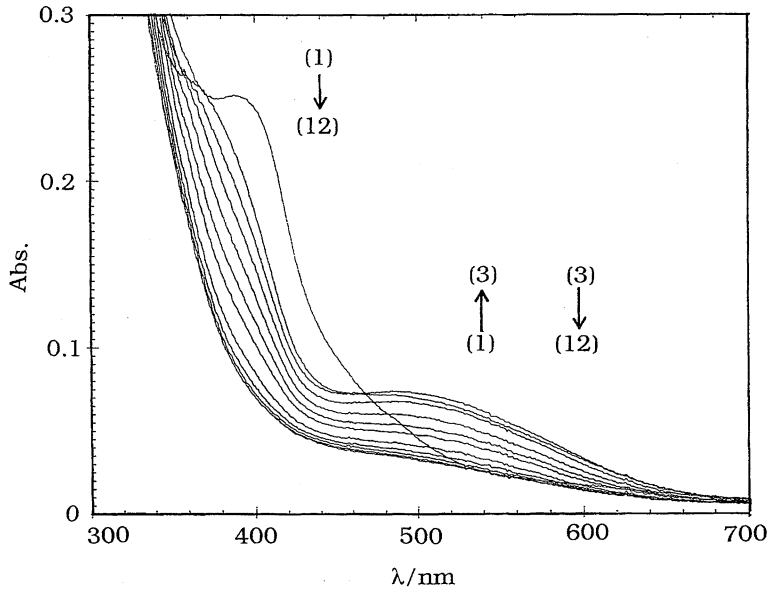

Fig. 5. Spectral changes in the H_2O_2 disproportionation catalyzed by [Mn(salen)Cl] in DMF at 25 °C. $[H_2O_2]_0 = 5.00\times10^{-2}$ mol dm^{-3}, $[[Mn(salen)Cl]]_0 = 5.00\times10^{-5}$ mol dm^{-3}, Time/min: (1) 0.5, (2) 5, (3) 10, (4) 15, (5) 30, (6) 45, (7) 90, (8) 120, (9) 150, (10) 210, (11) 270, (12) 360.

as $Mn^{IV}OH$, not $Mn^{IV}=O$, as described in the effect of the OH^- ion in the succeeding section. The $Mn^{IV}OH$ intermediate is formed by the reaction of Mn(III) with H_2O_2. The slow decreases in the absorbance after 15 min may be due to the decomposition of the catalyst to an inactive species, because decreases in H_2O_2 concentration were little observed after 150 min. Although the ESR spectrum at 77 K indicated a trace amount of the Mn(II) complex with a 6-line signal at $g=2$ in H_2O_2 disporoportionation, the presence of the $Mn^{IV}OH$ was not observed. A temperature lower than 77 K may be required for characterization of the Mn(IV) complex. A trace amount of the Mn(II) complex seems to be formed accompanying decomposition of the catalyst, althougth the characterization of an inactive species has not been carried out. From the above results, the mechanism of H_2O_2 disproportionation prior to decomposition of the catalyst is proposed as Scheme 1. The first step is the fast equilibrium of the Mn(III) complex and the $Mn^{IV}OH$ intermediate produced by the reaction of the Mn(III) complex with H_2O_2; the second step is followed by a slow reaction of the $Mn^{IV}OH$ intermediate with H_2O_2 to disproportionate O_2 and H_2O, recovering an original Mn(III) complex as the catalyst. From a steady-state method with respect to the $Mn^{IV}OH$ intermediate, we can obtain the following equation by using the equilibrium and rate constants defined in Scheme 1:

$$v = \frac{k_1 K_m [Mn(III)]_0^2 [H_2O_2]^2}{(1+\sqrt{K_m[H_2O_2]})^2}. \quad (1)$$

By rearranging Eq. 1, the following equation is derived:

$$\frac{[H_2O_2]_0}{\sqrt{v_0}} = \frac{1}{k_1 K_m [Mn(III)]_0} + \frac{\sqrt{[H_2O_2]_0}}{k_1 [Mn(III)]_0}, \quad (2)$$

where $[H_2O_2]_0$ and $[Mn(III)]_0$ are the initial concentrations. The plots of $[H_2O_2]_0/\sqrt{v_0}$ vs. $\sqrt{[H_2O_2]_0}$ at $[Mn(III)]_0=5.00\times10^{-5}$ mol dm^{-3} are linear, as shown in Fig. 6,

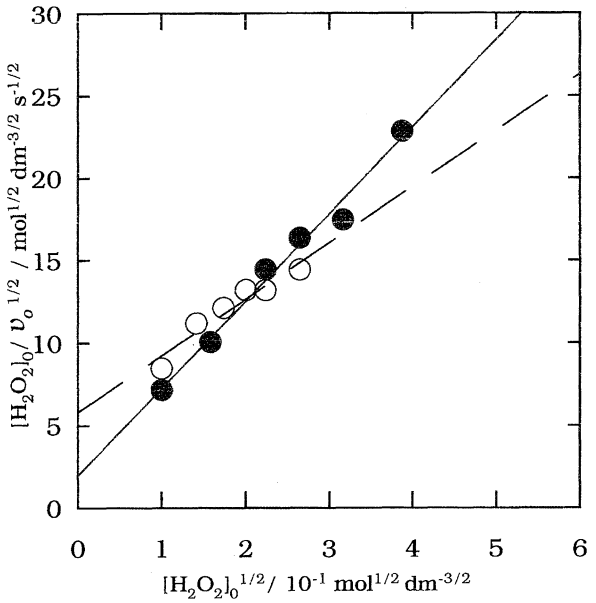

Fig. 6. The plots of $[H_2O_2]_0/\sqrt{v_0}$ vs. $\sqrt{[H_2O_2]_0}$ at $[Mn(III)]_0 = 5.00\times10^{-5}$ mol dm^{-3}. (●): [Mn(salen)Cl]; (○): [Mn(saltnOH)Cl].

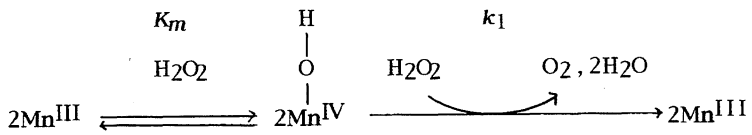

Scheme 1.

indicating that the proposed reaction mechanism is reasonable. Thus, the values of K_m and k_1 were obtained from the intercepts and slopes of the straight lines. The results are summarized in Table 1. The K_m and k_1 values decrease in the following order: [Mn(salen)Cl] > [Mn(saltnOH)Cl] > [Mn(saltn)Cl] > [Mn(saltnOCOPh)Cl], and [Mn(saltnOH)-Cl] > [Mn(salen)Cl] > [Mn(saltnOCOPh)Cl] > [Mn(saltn)Cl], respectively. Since the redox potentials in DMF are little influenced by the Mn(III) complex used, as shown in Table 1, the influence of ligands on the K_m and k_1 values is based on the structures of the Mn(III) complexes. The salen donor atoms and salen framework of $[Mn(salen)]^+$ in the crystal are coplanar to each other,[19] while the saltnOH framework for $[Mn(saltnOH)OCOCH_3]_n$ in the crystal is umbrella-shaped on account of the six-membered ring on the 1,3-diamine moiety.[20] Thus, saltn, saltnOH, and saltnOCOPh complexes with the six-membered ring may have similar distortions in DMF solution. The coordination of H_2O_2 to the distorted saltn, saltnOH, and saltnOCOPh complexes is more difficult than that of the distorted-free salen complex, resulting in the distorted Mn(IV) intermediate being unstable compared with the distorted-free Mn(IV) intermediate. Thus, the K_m values may decrease with increasing distortion of the Mn(III) complexes. In spite of the small K_m values for the distorted saltn, saltnOH, and saltnOCOPh complexes relative to the distorted-free salen complex, as shown in Table 1, the k_1 value for the distorted saltnOH complex is larger than that for the distorted-free salen complex. Except for the distorted-free salen complex, the k_1 values increase in the order saltn < saltnOCOPh < saltnOH in accordance with the increase of the hydrogen-bonding ability on ligands. This strongly suggests stabilization of the transition state due to the formation of hydrogen-bondings between the $Mn^{IV}OH$ intermediates and H_2O_2 as proposed in Fig. 7.

Effect of Hydroxide Ion on H_2O_2 Disproportionation by [Mn(salen)Cl]. The effect of the OH^- ion on H_2O_2 disproportionation by [Mn(salen)Cl] in DMF was examined under two reaction conditions: $[OH^-]_0=(0.18-22.3)\times10^{-4}$ mol dm^{-3} at $[H_2O_2]_0=5.00\times10^{-2}$ mol dm^{-3} and $[Mn(III)]_0=5.00\times10^{-5}$ mol dm^{-3} (Type A: further addition of the OH^- ion to preceding reaction conditions in the absence of the OH^- ion) and $[OH^-]_0=(0.6—4.80)\times10^{-4}$ mol dm^{-3} at $[H_2O_2]_0=5.00\times10^{-3}$ mol dm^{-3} and $[Mn(III)]_0=2.00\times10^{-4}$ mol dm^{-3} (Type B). The correlation between v_0 and $[OH^-]_0$ is shown for Types A and B in Figs. 8(a) and 8(b), respectively. For Type A, the v_0 value increases with increasing $[OH^-]_0$, and finally reaches a constant. For Type B, the v_0 value is linear to the second order in $[OH^-]_0$. The spectral changes for Type A are quite different from that for Type B, as shown in Figs. 9(a) and 9(b), respectively. For Type A, after a few minutes the reddish-yellow solution turned reddish purple and exhibited an intense absorption band characteristic of the $Mn^{IV}=O$ complex near to 520 nm for a long time. The fine structure is assigned to the $\nu(Mn^{IV}=O)$ vibration coupled to the LMCT band through any vibronic interaction.[15,16,28,29] It is reasonable that in contrast to the $Mn^{IV}OH$ intermediate formed in the absence of the OH^- ion, deprotonated $Mn^{IV}=O$

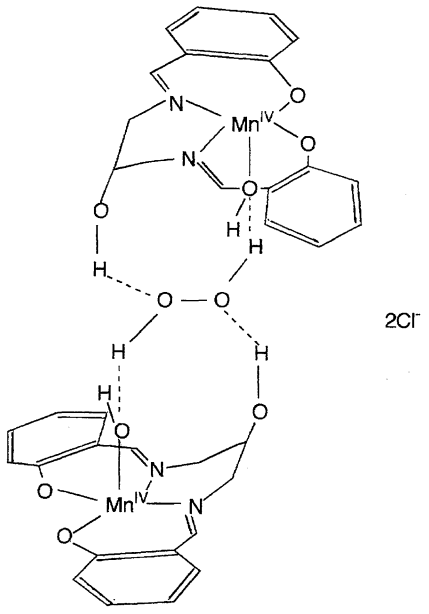

Fig. 7. Proposed transition state structure for [Mn(saltnOH)Cl].

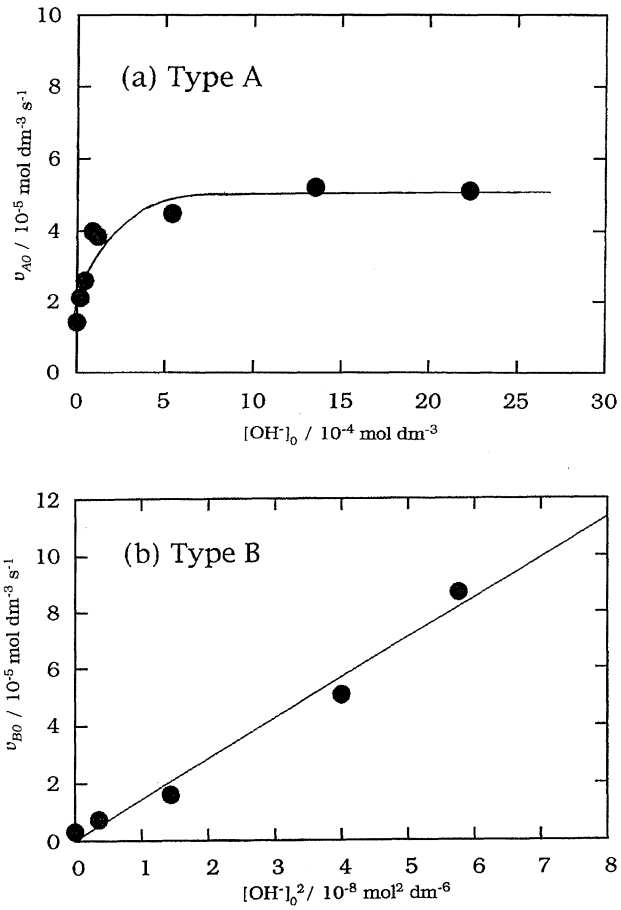

Fig. 8. The correlation between v_0 and the OH^- ion concentrations for (a) Type A and (b) Type B. (a) Type A: $[H_2O_2]_0 = 5.00\times10^{-2}$ mol dm^{-3}, $[[Mn(salen)Cl]]_0 = 5.00\times10^{-5}$ mol dm^{-3}; (b) Type B: $[H_2O_2]_0 = 5.00\times10^{-3}$ mol dm^{-3}, $[[Mn(salen)Cl]]_0 = 2.00\times10^{-4}$ mol dm^{-3}.

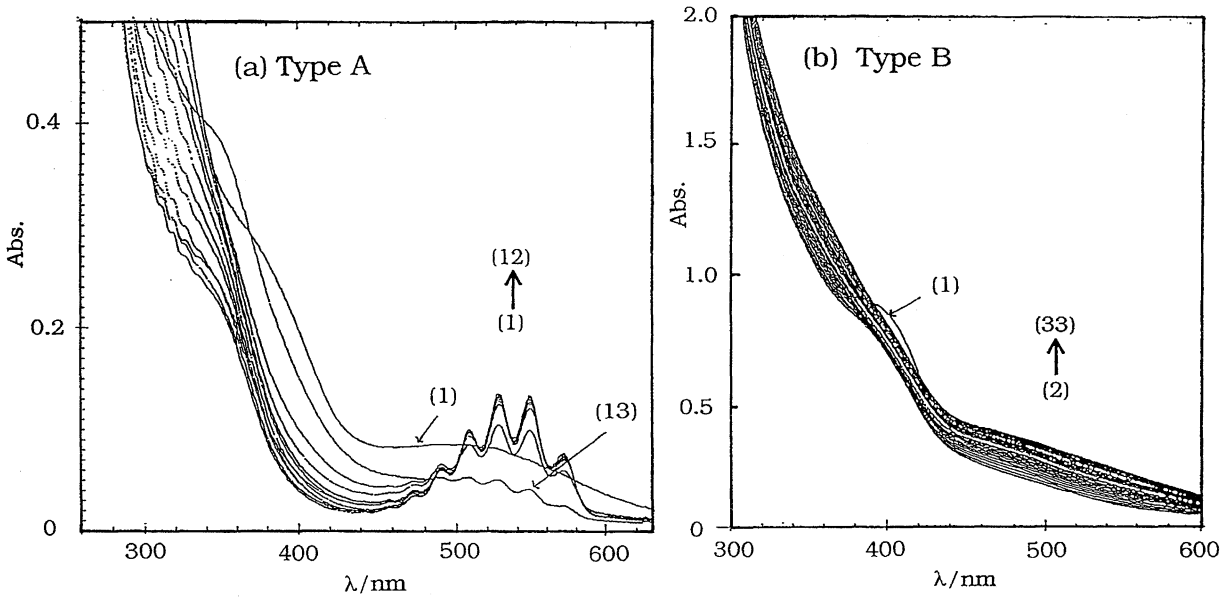

Fig. 9. Spectral changes in the H_2O_2 disproportionation catalyzed by [Mn(salen)Cl] in DMF at 25 °C for (a) Type A and (b) Type B. (a) Type A: $[H_2O_2]_0=5.00\times10^{-2}$ mol dm^{-3}, $[[Mn(salen)Cl]]_0=5.00\times10^{-5}$ mol dm^{-3}, $[OH^-]_0=2.20\times10^{-3}$ mol dm^{-3}, Time/min; (1) 0.5, (2) 5, (3) 10, (4) 15, (5) 20, (6) 30, (7) 45, (8) 60, (9) 90, (10) 120, (11) 150, (12) 270, (13) 360. (b) Type B: $[H_2O_2]_0=5.00\times10^{-3}$ mol dm^{-3}, $[[Mn(salen)Cl]]_0=2.00\times10^{-4}$ mol dm^{-3}, $[OH^-]_0=1.20\times10^{-4}$ mol dm^{-3}, Time; (1)—(33) per 5 min.

appears in the presence of the OH^- ion. Moreover, the ESR signal did not show any trace amont of the Mn(II) complex in the presence of the OH^- ion. On the other hand, for Type B, the later spectra in H_2O_2 disproportionation resemble that of the dinuclear Mn complex bridged by O_2.[30,31] The time dependence of O_2 evolution by [Mn(salen)Cl] in the absence and presence of the OH^- ion is shown in Fig. 2. In the absence of the OH^- ion, O_2 evolution gradually increases with time. However, in the presence of the OH^- ion, O_2 evolution at the early stage occurs vigorously; then, O_2 consumption is slowly followed, suggesting that a compound active toward O_2 is formed during disproportionation. The ESR spectrum of Type B in Fig. 10(b) shows a 6-line signal with $g\fallingdotseq2$ in the 300—350 mT range, indicating the formation of the Mn(II) complex. In addition to this signal, a fine 6-line signal can be seen in the 320—330 mT range. Although the formation of an organic radical is suggested, the fine signal may be due to the Mn(III)–O_2^- intermediate[30] produced by the reaction of the Mn(II) with O_2. The fine signal for Co(III)–O_2^- also appears at $g\fallingdotseq2$.[27,32] A significant decrease in the base line with increasing magnetic field is often observed for vigorous O_2 evolution. From the above results, it is concluded that

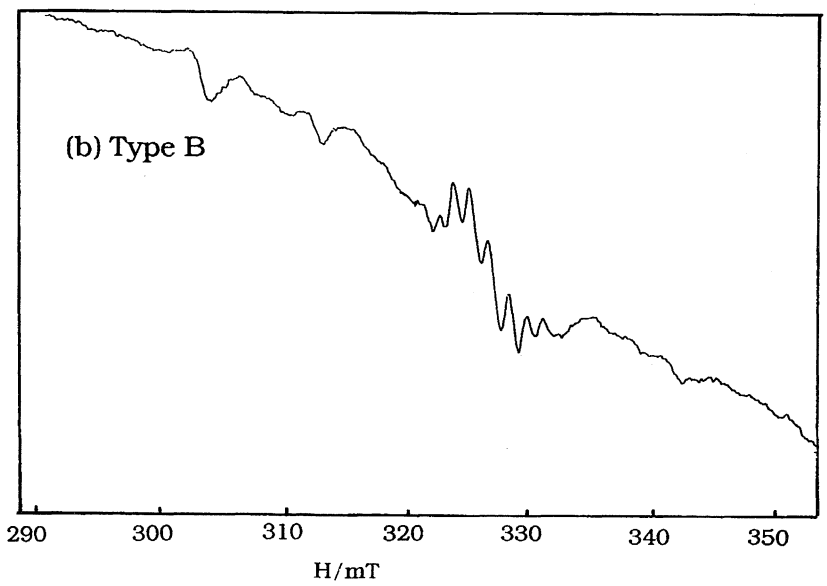

Fig. 10. ESR spectrum on the frozen DMF solution (77 K) for Type B. $[H_2O_2]_0=5.00\times10^{-3}$ mol dm^{-3}, $[[Mn(salen)Cl]]_0=2.00\times10^{-4}$ mol dm^{-3}, $[OH^-]_0=2.00\times10^{-4}$ mol dm^{-3}.

the intermediate for Type B is the Mn(II) complex.

The effect of the OH^- ion on H_2O_2 disproportionation may be mainly ascribed to two cases: One is the acceleration of the proton dissociation by OH^- ion on H_2O_2; the other is coordination of the OH^- ion to the Mn(III) complex. Since the basicity in H_2O_2 is large in DMF, the dissociation of proton on H_2O_2 is negligibly small in the range of the OH^- concentrations used.[33] On the other hand, the complexation between the $[Mn(salen)]^+$ and the OH^- ion was confirmed by calorimetry and the value of $\log K_1$ was estimated to be about 2—3.[34] The $[Mn(salen)]^+$ solution in the presence of the OH^- ion showed little spectral change under the OH^- concentration used, indicating that the dinuclear Mn(III) complex is not formed in solution.[30] Therefore, in the presence of the OH^- ion, the disproportionation mechanisms are proposed as Scheme 2 (Type A) and Scheme 3 (Type B). For Type A, disproportionation produces the Mn^{IV}=O intermediate and again recovers the $Mn^{III}OH$ complex. The reaction may proceed by both Schemes 1 and 2 under a lower OH^- concentration. Because $Mn^{III}OH$ is almost formed above $[OH^-]_0=1\times10^{-3}$ mol dm^{-3}, the reaction occurs via only Scheme 2 above $[OH^-]_0=1\times10^{-3}$ mol dm^{-3}. Thus, we can obtain the following equation under the condition of $[Mn(III)]_0=5\times10^{-5}$ mol dm$^{-3}\ll[OH^-]_0=1\times10^{-3}$ mol dm^{-3}:

$$v_A = k_2[Mn(III)]_0^2[H_2O_2]. \quad (3)$$

In fact, since v_{A0} is independent of the OH^- concentration above $[OH^-]_0=1\times10^{-3}$ mol dm^{-3}, as shown in Fig. 8(a), the value of $k_2=3.85\times10^5$ mol^{-2} dm^6 s^{-1} is obtained. For Type B, the $Mn^{III}OH$ coordinated by the OH^- ion disproportionates H_2O_2 to O_2 and H_2O, producing the Mn(II) complex. When an excess of H_2O_2 is present in solution, the Mn(II) complex produced reacts rapidly with H_2O_2 to recover the $Mn^{III}OH$. Once H_2O_2 is almost consumed, the dinuclear Mn complex bridged by O_2 may be slowly formed under the reaction condition used. By using the equilibrium constant, $K_{OH}=10^2$—10^3 mol^{-1} dm^3 and the rate constant defined by Scheme 3 under the conditions $[OH^-]_0<4\times10^{-4}$ mol dm^{-3} and $[Mn^{III}]<2\times10^{-4}$ mol dm^{-3}, the rate (v_B) can be written as

$$v_B = 2k_3K_{OH}[Mn(III)]_0^2[OH^-]_0^2[H_2O_2]. \quad (4)$$

The k_3 value is estimated to be $3.6\times(10^9$—$10^{10})$ mol^{-2} dm^6 s^{-1} from the slope of the plot of v_{B0} vs. $[OH^-]_0^2$ (Fig. 8(b)).

The H_2O_2 disproportionation catalyzed by the Mn(III) complex consists of the half reactions of the following Eqs. 5, 6, 7, 8, and 9 with the standard redox potential E value:

$$H_2O_2 + 2H^+ + 2e^- \rightleftarrows 2H_2O \qquad E_{H_2O_2} \quad (5)$$

$$Mn^{IV}OH + H^+ + e^- \rightleftarrows Mn^{III} + H_2O \qquad E_1 \quad (6)$$

$$Mn^{IV}{=}O + H^+ + e^- \rightleftarrows Mn^{III}OH \qquad E_2 \quad (7)$$

$$Mn^{III}OH + H^+ + e^- \rightleftarrows Mn^{II} + H_2O \qquad E_3 \quad (8)$$

$$O_2 + 2H^+ + 2e^- \rightleftarrows H_2O_2 \qquad E_{O_2} \quad (9)$$

In the absence of the OH^- ion, the reaction proceeds by the Mn(III)–Mn(IV) cycle coupled with Eqs. 5, 6, and 9. As shown in Fig. 11, the potentials of Mn(III)–Mn(IV) coupled near to +0.5 V are shifted to more negative values with the addition of the OH^- ion. Accordingly, the formation of $Mn^{III}OH$ causes a smaller difference between the potentials of the Mn(III)–Mn(II) and the Mn(IV)–Mn(III) couples. If either $(E_3-E_{O_2})\ll(E_{H_2O_2}-E_2)$ or $(E_3-E_{O_2})\gg(E_{H_2O_2}-E_2)$, the reaction would occur only by either the Mn(III)–Mn(IV) or Mn(II)–Mn(III) cycle, irrespective of the reaction conditions, respectively. In the present investigation, the appearance of either the Mn(III)–Mn(IV) cycle (Type A) or the Mn(II)–Mn(III) cycle (Type B) according to the reaction conditions strongly suggests $(E_3-E_{O_2})\fallingdotseq(E_{H_2O_2}-E_2)$ based on the formation of $Mn^{III}OH$.

Comparison of Functional Models for Mn Catalases. The reaction rates, Mn redox cycles, and Mn–Mn distances for functional model Mn complexes which include mononuclear and dinuclear Mn centers are shown in Table 2.[36] The reaction rates are normalized by $v_0/[Mn(III)]_0$ because the reaction order depends on the Mn complexes used. Among the mononuclear complexes, the catalase-like activities for Schiff base mononuclear Mn(III) complexes, expect for [Mn(saltn)Cl], are large compared with those for $[Mn(TPP)]^+$[17] and $[Mn(H_2O)_6]^{2+}$.[10] Moreover, the catalase-like activity for mononuclear [Mn(salen)OH] with the Mn(II)–Mn(III) cycle

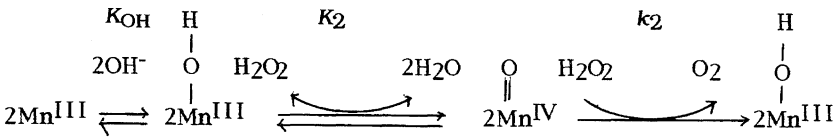

Scheme 2. (Type A).

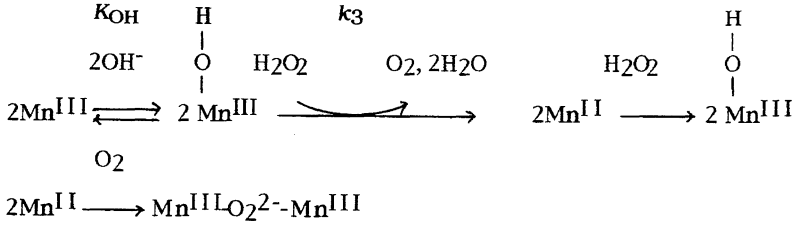

Scheme 3. (Type B).

Table 2. Comparison of Functional Models for Mn Catalase

Catalyst	Rate/s^{-1}	Mn-redox cycle	Mn–Mn distance/Å	Refs.
Mn catalase	2.0×10^5	(II,II)–(III,III)	3.6	35
$[Mn^{IV}(saltn)(\mu\text{-}O)]_2$	50	(III,III)–(IV,IV)	2.73	8, 9, 36
$[Mn^{III}(saltnO)]_2$	13	(II,II)–(III,III)	3.33	10, 36
$[Mn_2L]Cl_2$ (L = anthracenediporphyrin)	5.4	(III,III)–(IV,IV)	4.5	17
$[Mn^{II}L(CH_3COO)](ClO_4)_2$ (L = *N*,*N*,*N*′,*N*′-tetrakis-(2-methylene-benzimidazolyl-)-1,3-diaminopropan-2-ol)	3.71	(II,II–III,III)	3.3	13
$[Mn_2L(C_6H_5COO)_2(NCS)]$ (L = 2,6-bis(*N*-(2-(dimetylamino)ethyl) iminomethyl)-4-methylphenolate) (L*m*,*n* = (CH_2) *m*,*n*-bis(2,6-bis(*N*-(2-(dimetyl-amino)ethyl)iminomethyl)-4-methylphenolate)	0.79	(III,III–IV,IV)	3.325	14, 15
[Mn(salen)OH][a)]	24	II–III		This work
[Mn(salen)OH][a)]	1.2	III–IV		This work
[Mn(saltnOH)Cl]	0.54	III–IV		This work
[Mn(salen)Cl]	0.24	III–IV		This work
[Mn(saltnOCOPh)Cl]	0.033	III–IV		This work
[Mn(saltn)Cl]	0.009	III–IV		This work
[Mn(TPP)Cl]	0.013	III–V		17
$[Mn(H_2O)_6](ClO_4)_2$	0.0063	Unknown		10

a) At $[OH^-]_0=0.002$ mol dm^{-3}.

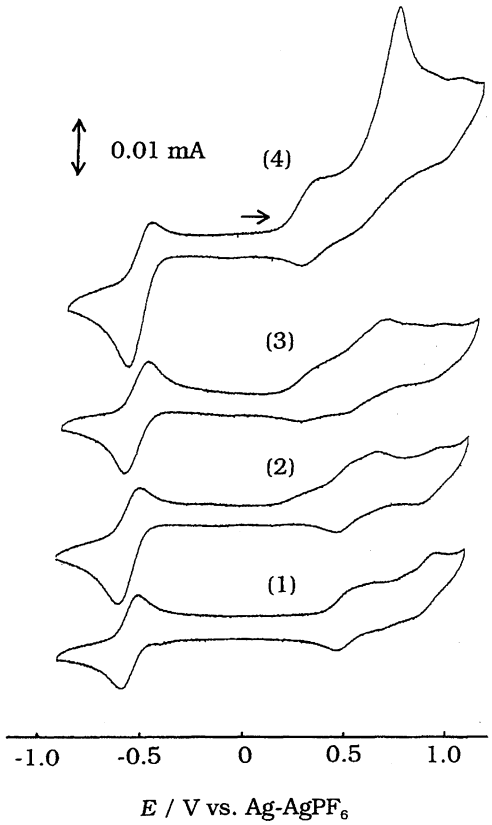

Fig. 11. The OH^- concentration dependence on the cyclic voltammograms of [Mn(salen)Cl]. $[[Mn(salen)Cl]]_0 = 1.00\times10^{-3}$ mol dm^{-3}, $[OH^-]_0/10^{-3}$ mol dm^{-3}: (1) 0, (2) 0.50, (3) 1.0 (4) 2.0.

is comparable to that for the dinuclear $[Mn(saltnO)]_2$ with the Mn(II)–Mn(III) cycle and the dinuclear $[Mn(saltn)(\mu\text{-}O)]_2$ with the Mn(III)–Mn(IV) cycle.[10] The activities may be affected not only by the redox potentials of the Mn(III) complexes used, but also by the reaction site of the Mn(III) complex by H_2O_2. An attack of H_2O_2 to the Mn(III) complex may easily occur in the outer sphere compared with that in the inner sphere, which is accompanied by solvent substitution by H_2O_2 on the Mn(III) complexes. For mononuclear [Mn(salen)OH] and dinuclear $[Mn(saltn)(\mu\text{-}O)]_2$ complexes with high activities, they undergo an H_2O_2 attack at the OH group on the [Mn(salen)OH] during the first step, as shown in Scheme 3, and at two μ-oxo sites on the dinuclear $[Mn(saltn)(\mu\text{-}O)]_2$ complex,[8,9] respectively. The dinuclear $[Mn(saltnO)]_2$ may have an H_2O_2 attack similar to the dinuclear $[Mn(saltn)(\mu\text{-}O)]_2$ complex. However, the reactions for the mononuclear [Mn(saltn)Cl] and [Mn(saltnOH)Cl] complexes proceed via the coordination of H_2O_2 to the Mn(III) complex, as shown in Scheme 1. This seems to be one reason why the activities for the dinuclear $[Mn(saltn)(\mu\text{-}O)]_2$ and $[Mn(saltnO)]_2$ are higher than those for the mononuclear [Mn(saltn)Cl] and [Mn(saltnOH)Cl]. However, Mn-CAT from *L. Plantarum* exhibits a 10^5 faster rate than the Mn complexes with the best functinal mode.[35] Dismukes et al. have pointed out that the active site of Mn-CAT from *T. thermophilus* possesses protein residues with the two donor and acceptor protons required for the redox reaction of H_2O_2, and that the lack of proton donor and acceptor groups near to the catalytic site for synthetic Mn complexes may be the reason for the intense suppression of the rate compared to the

Mn-CAT.[12] In the present study, the existence of the hydroxy group with the property of a proton donor on the 1,3-diamine ring leads to an increased rate on account of the formation of hydrogen-bonding. The proton donor and acceptor groups appear to play an important role in the catalase-like activities.

The authors acknowledge Prof. Hiromu Sakurai of Kyoto Pharmaceutical University for the measurement of ESR spectra.

References

1) a) "Bioinorganic Chemistry," ed by D. P. Kessissoglou, Kluwer Academic Publishers, The Haque (1995), p. 299; b) V. L. Pecoraro, M. J. Baldwin, and A. Gelasco, *Chem. Rev.*, **94**, 807 (1994).

2) a) G. C. Dismukes, *Photochem. Photobiol.*, **43**, 99 (1986); b) R. J. Debus, *Biochim. Biophys. Acta*, **1102**, 269 (1992); c) I. I. Putrenko, *Biochemistry*, **35**, 2865 (1996).

3) K. A. Pattrige, R. K. Strong, and M. L. Ludwig, *J. Biol. Chem.*, **260**, 16426 (1985).

4) *Lactobacillus plantarum*: a) Y. Kono and I. Fridovich, *J. Biol. Chem.*, **258**, 13646 (1983); b) W. F. Beyer, Jr., and I. Fridovich, *Biochemistry*, **24**, 6460 (1985). *Thermus thermophilus*: c) V. V. Barynin and A. I. Grebenko, *Dokl. Acad. Nauk SSSR*, **286**, 461 (1986). *Thermoleophilum album*: d) G. S. Allgood and J. J. Perry, *J. Bacteriol.*, **168**, 563 (1986).

5) V. V. Barynin, A. A. Vagin, V. R. Melik-Adamyan, A. I. Grebenko, S. V. Khangulov, A. V. Popov, M. E. Andrianova, and A. B. K. Vainshtein, *Sov. Phys.-Dokl.*, **31**, 457 (1986).

6) S. V. Khangulov, V. V. Barynin, V. R. Melik-Adamyan, A. I. Grebenko, N. V. Voyevodskaya, L. A. Blumenfeld, S. N. Dobryakov, and V. B. Il'Yasova, *Bioorg. Khim.*, **12**, 741 (1986).

7) G. S. Waldo, S. Yu, and J. E. Penner-Hahn, *J. Am. Chem. Soc.*, **114**, 5869 (1992).

8) E. J. Larson and V. L. Pecoraro, *J. Am. Chem. Soc.*, **113**, 3810 (1991).

9) E. J. Larson and V. L. Pecoraro, *J. Am. Chem. Soc.*, **113**, 7809 (1991).

10) A. Gelasco and V. L. Pecoraro, *J. Am. Chem. Soc.*, **115**, 7928 (1993).

11) P. Mathur, M. Crowder, and G. C. Dismukes, *J. Am. Chem. Soc.*, **109**, 5227 (1987).

12) P. J. Pessiki, S. V. Khangulov, D. M. Ho, and G. C. Dismukes, *J. Am. Chem. Soc.*, **116**, 891 (1994).

13) P. J. Pessiki and G. C. Dismukes, *J. Am. Chem. Soc.*, **116**, 898 (1994).

14) H. Sakiyama, H. Okawa, and R. Isobe, *J. Chem. Soc., Chem. Commun.*, **1993**, 882.

15) H. Sakiyama, H. Tamaki, M. Kuroda, N. Matsumoto, and H. Okawa, *J. Chem. Soc., Dalton Trans.*, **1993**, 591.

16) H. Wada, K. Motoda, M. Ohba, H. Sakiyama, N. Matsumoto, and H. Okawa, *Bull. Chem. Soc. Jpn.*, **68**, 1105 (1995).

17) Y. Naruta and K. Maruyama, *J. Am. Chem. Soc.*, **113**, 3595 (1991).

18) Y. Naruta, M. Sasayama, and K. Maruyama, *Chem. Lett.*, **1992**, 1267.

19) V. L. Pecoraro and W. M. Butler, *Acta Crystallogr., Sect. C*, **C42**, 1151 (1986).

20) J. A. Bonadies, M. L. Kirk, M. S. Lah, D. P. Kessissoglou, W. E. Hatfield, and V. L. Pecoraro, *Inorg. Chem.*, **28**, 2037 (1989).

21) R. H. Holm, G. W. Everett, and A. Charkavorty, *Prog. Inorg. Chem.*, **7**, 82, (1966).

22) Y. Abe, K. Morikawa, and M. Kikukawa, *Polyhedron*, **7**, 2135 (1988).

23) Y. Abe, M. Uehara, A. Ueda, and N. Sakagami, "The 45th Symposium on Coordination Chemistry of Japan," Fukuoka, November 1995, Abstr., p. 178.

24) B. Bosnich, *J. Am. Chem. Soc.*, **90**, 627 (1968).

25) R. S. Downing and F. L. Urbach, *J. Am. Chem. Soc.*, **91**, 5977 (1969).

26) J. Balla, T. Kiss, and R. F. Jameson, *Inorg. Chem.*, **31**, 58 (1993).

27) H. Sakurai, "Practice of Electron Spin Resonace Spectrum," Hirokawa Publishing Co., Tokyo (1992).

28) R. S. Czernuszewicz, Y. O. Su, M. K. Stern, K. A. Macor, D. Kim, J. T. Groves, and T. G. Spiro, *J. Am. Chem. Soc.*, **110**, 4158 (1988).

29) H. B. Gray, *Coord. Chem. Rev.*, **1**, 2 (1996).

30) T. Matsushita, T. Yarino, I. Masuda, T. Shono, and K. Shinra, *Bull. Chem. Soc. Jpn.*, **46**, 1712 (1973).

31) L. J. Boucher and C. G. Coe, *Inorg. Chem.*, **14**, 1289 (1975).

32) T. Yonetani, H. Yamamoto, and T. Iizuka, *J. Biol. Chem.*, **249**, 2168 (1974).

33) The value of pK_1 for H_2O_2 in DMF solution was estimated to be 13.86 by potentiometric titration.

34) The precipitate was deposited from DMF solution at [Mn(III)]$_0 > 5\times10^{-3}$ mol dm^{-3} during the calorimetric titration. Because the calorimetry was performed at [Mn(III)]$_0 < 5\times10^{-3}$ mol dm^{-3}, the K_1 value for [Mn(salen)OH] was obtained with some uncertainty.

35) J. E. Penner-Hahn, in "Manganese Redox Enzymes," ed by V. L. Pecoraro, VCH Publishers, Inc., New York (1992).

36) V. L. Pecoraro, M. J. Baldwin, and A. Gelasco, *Chem. Rev.*, **94**, 807 (1994).